# Subzero Temperature-Induced Lattice Compression Enables High Carrier Mobility in $MAPbBr_3$ Single Crystals.

## Supporting Information.

*Tehinke Achille Malo, Xin Xu, Min Soo Kim, Dong Hwan Wang*, and Aung Ko Ko Kyaw**

T. A. Malo, X. Xu, A. K. K. Kyaw

Department of Electronic & Electrical Engineering

Southern University of Science and Technology, Shenzhen 518055, P. R. China

E-mail: aung@sustech.edu.cn

M. S. Kim, D. H. Wang

School of Integrative Engineering, Chung-Ang University, 84 Heukseok-ro, Dongjak-gu, Seoul 06974, Republic of Korea

E-mail : king0401@cau.ac.kr

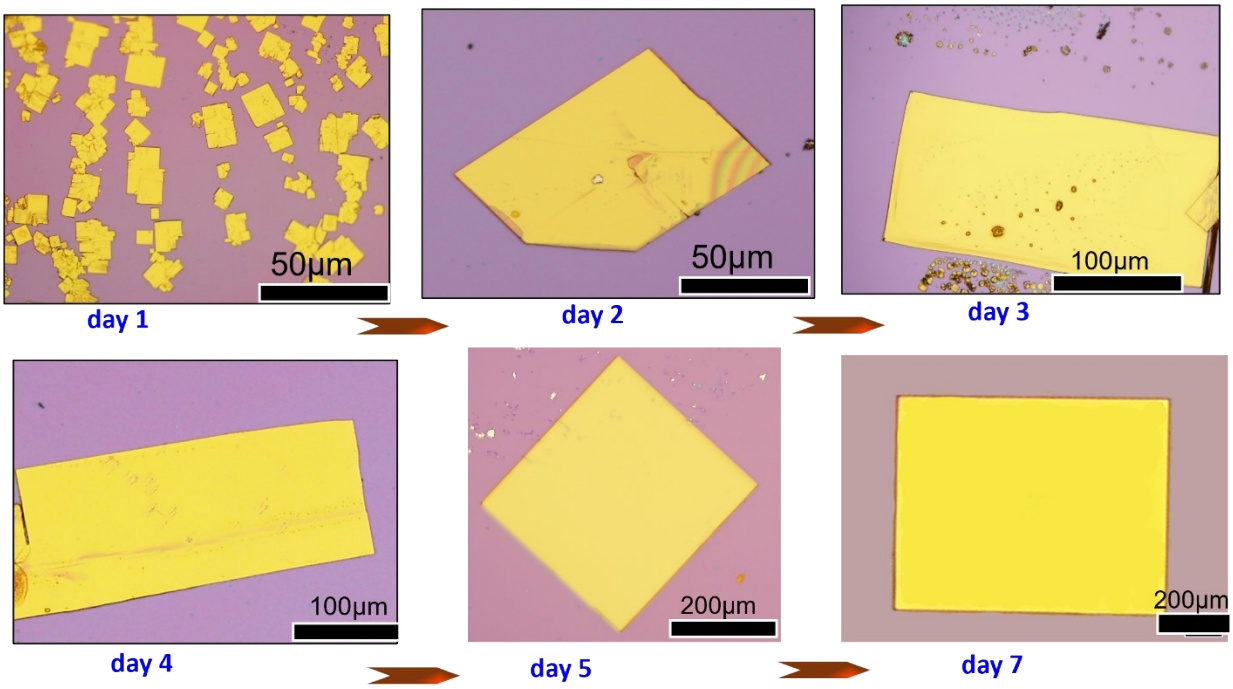


**Figure S1.** Crystal Growth Rate and Control. T = -18 °C; Concentration (C)= 0.25 M, DMF/GBL. The crystal size increases with the growing time (number of days). A $MAPbBr_3$ micro flake was obtained on day 7.

The perovskite crystallization mechanism is complex and can involve several steps and intermediate species. The complexity arises from the fact that perovskites can form through various pathways and can involve multiple chemical reactions, phase transitions, and nucleation and growth processes[1-3]. Perovskite solubility is highly dependent on temperature, and it typically increases with increasing temperature until it reaches a saturation point beyond which no more perovskites can dissolve in the solvent. The solubility curve typically exhibits a maximum at an intermediate temperature, beyond which the solubility decreases with increasing temperature. This behavior is known as retrograde solubility and is attributed to changes in the solvent's properties at higher temperatures that affect its ability to dissolve perovskite[4]. The optimum temperature range for perovskite crystallization depends on the specific type of perovskite and the solvent used. Generally, the temperature range for perovskite crystallization is above the solubility curve's maximum and below the point where the perovskite starts to decompose. This temperature range is typically between 60 and 150° C for most perovskite materials, including all solvents. The

solubility curve of perovskites established by previous research as a function of temperatures shows high solubility at lower temperatures and lower solubility at high temperatures[4]. In contrast to the typical behavior of perovskite retrograde solubility[4], where solubility decreases with increasing temperatures, our study revealed a contradictory trend. We observed that under freezing temperatures (below zero degrees Celsius), the solubility of the perovskite solution decreased with a decrease in temperature. Unlike the retrograde solubility commonly observed with increasing temperatures, where solubility decreases, we found that the perovskite solution exhibited forward solubility when it was subjected to temperatures below its equilibrium temperature. This means that the solubility of the perovskite solution decreased as the temperature decreased, contrary to the expected behavior. This phenomenon highlights the importance of considering the specific conditions and temperature ranges when studying the solubility and crystallization behavior of perovskite solutions. While the exact mechanisms governing the solubility behavior of perovskite solutions at freezing temperatures require further investigation, our findings provide evidence of a non-conventional solubility trend for perovskite materials. This highlights the complexity of perovskite solubility and crystallization phenomena and emphasizes the importance of exploring different temperature regimes and solvent combinations to fully understand and optimize the growth of perovskite crystals. By recognizing and addressing this contradiction, we have contributed to the body of knowledge surrounding perovskite solubility and crystallization behavior, and our findings may inspire further research and exploration in this area.

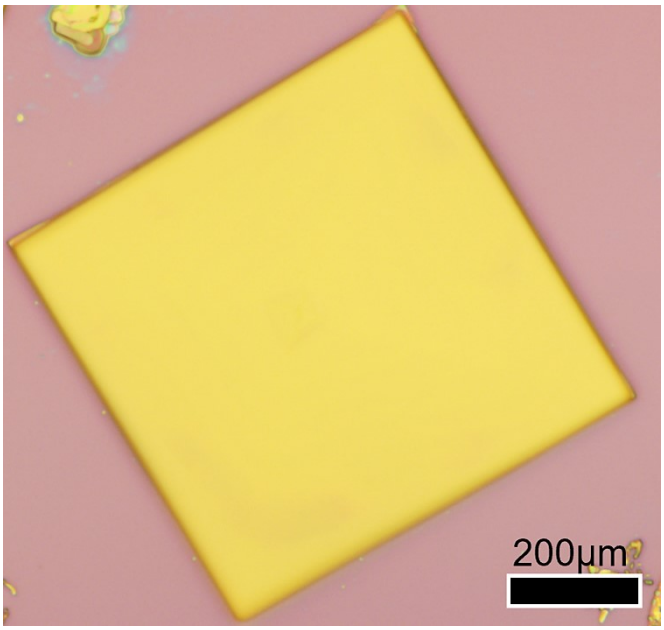


**Figure S2.** High-temperature $CH_3NH_3PbBr_3$ Single Crystal micro flake. T = 80 °C;  C= 0.25 M, DMF.

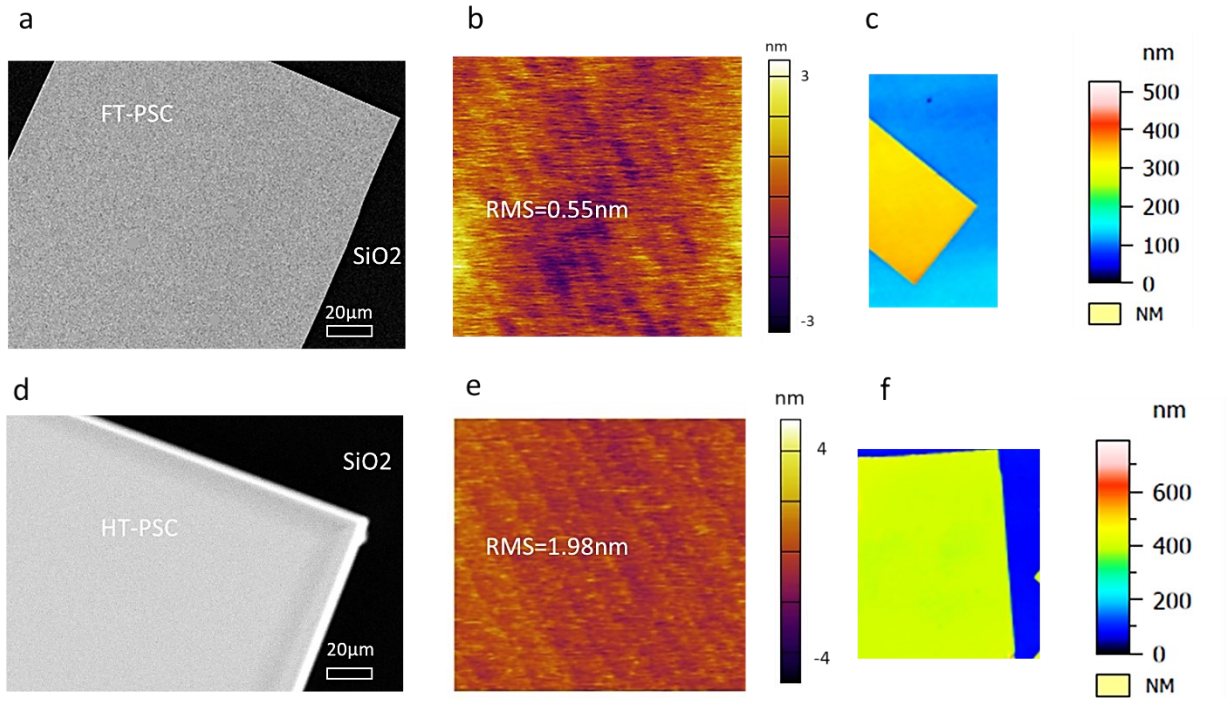


**Figure S3: Morphology of FT and HT PSCs.** (a, d) SEM images of FT PSC and HT PSC respectively. Scale bar 20µm. (b, e) AFM image of FT PSC and HT PSC, respectively. (c,f) 3D optical microscopy images of FT and HT PSCs, respectively. FT PSC average thickness was 316 nm while that of the HT PSC was 320 nm. The intensity scale bar in nm indicates the crystal thickness.

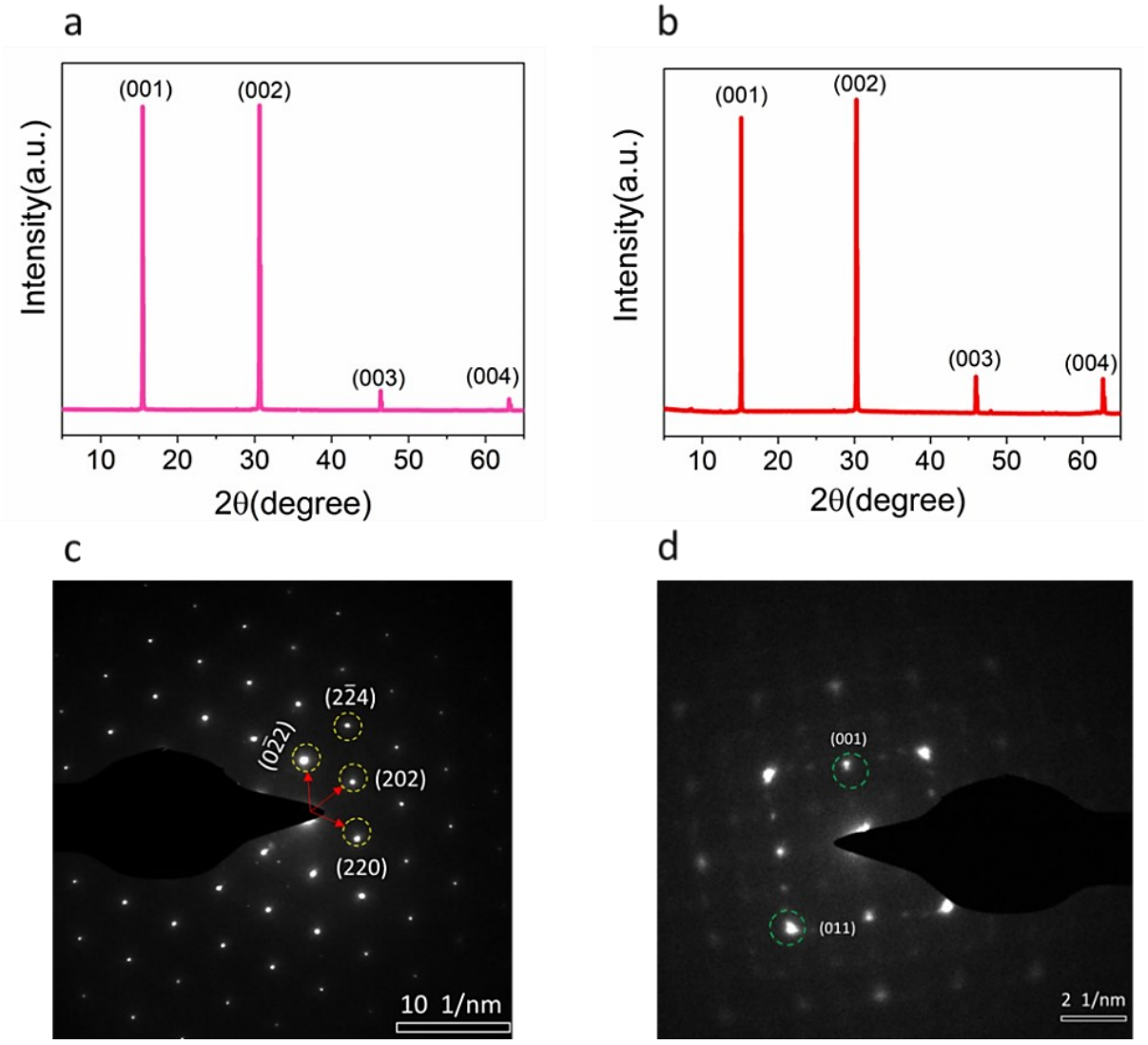


**Figure S4: Structural features of FT and HT PSCs**. (a-b) XRD patterns of FT PSC and HT PSC, respectively. (c-d) SAED TEM diffraction pattern of FT PSC and HT PSC, respectively.

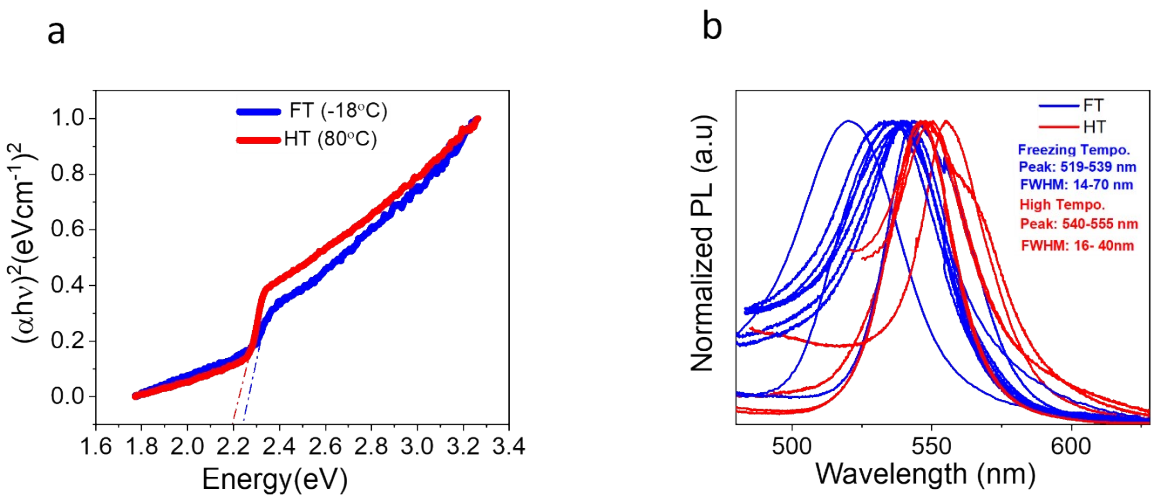


**Figure S5: Assessment of the optoelectronic characteristics.** (a) Tauc plot analysis of the absorption spectra of FT PSC (-18° C) and HT PSC. (b) PL spectra of FT PSC and HT PSC.

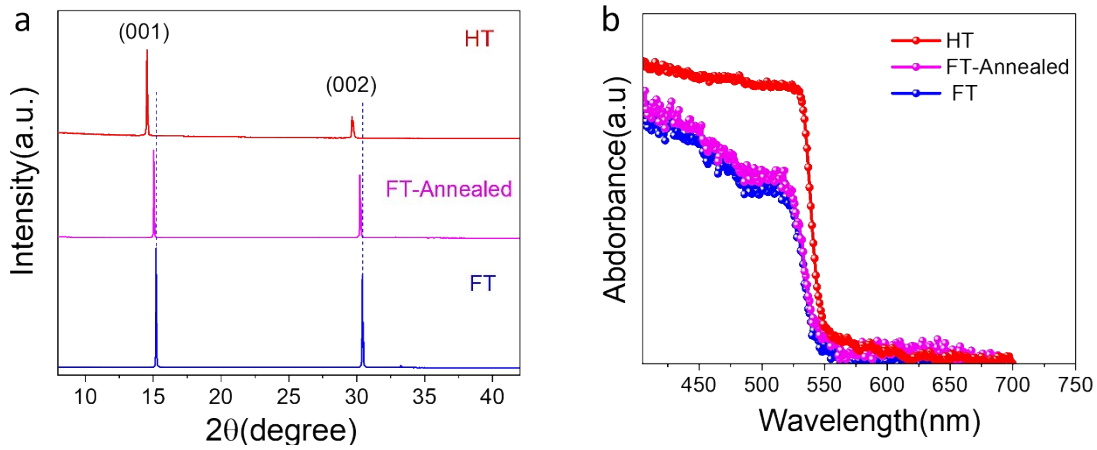


**Figure S6.** Thermal stability of freezing-temperature–induced lattice compression in $MAPbBr_3$ single crystals. Left: XRD patterns of HT-grown (red), FT-grown (blue), and FT-annealed (magenta) $MAPbBr_3$ single crystals after a heating–cooling cycle at 80 °C.

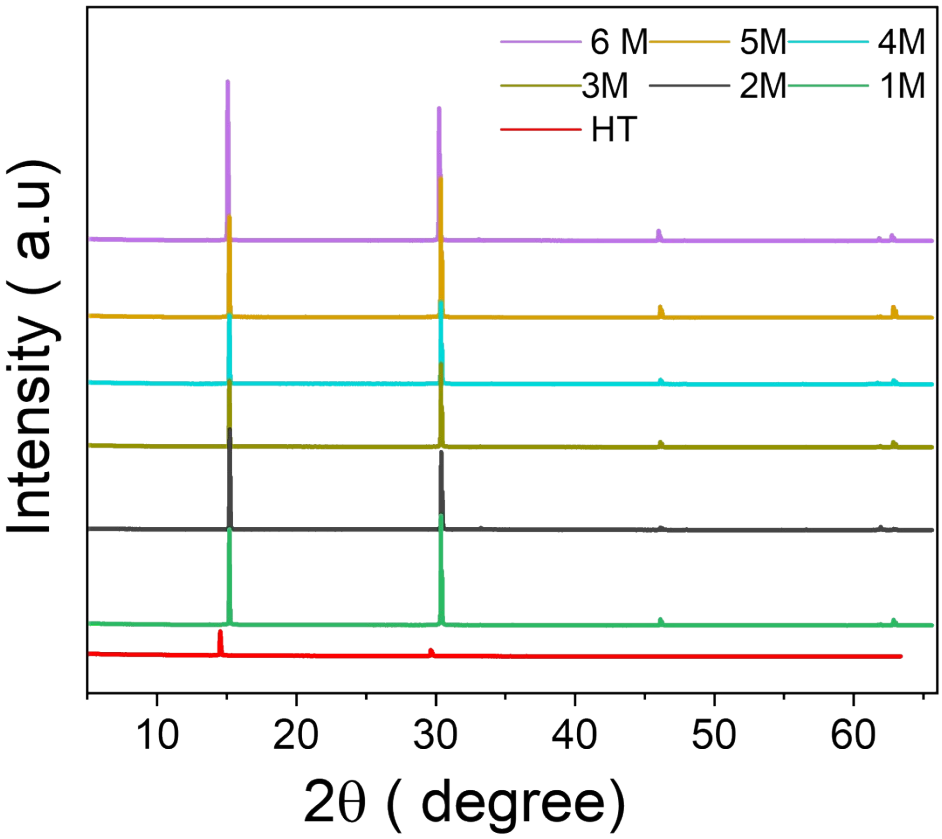


**Figure S7:** XRD patterns of freezing-temperature (FT) grown $MAPbBr_3$ single crystals collected over a period of 6 months (M1–M6, where M denotes months.

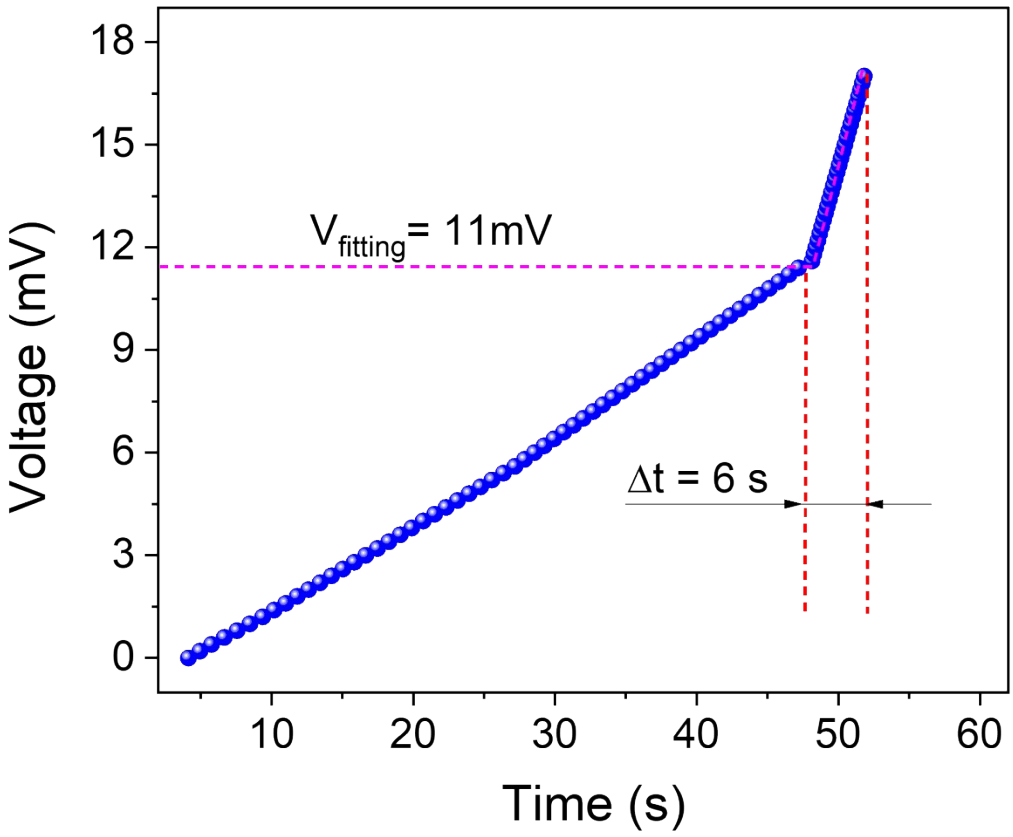


Figure S8. Time–voltage profile used for SCLC measurements.

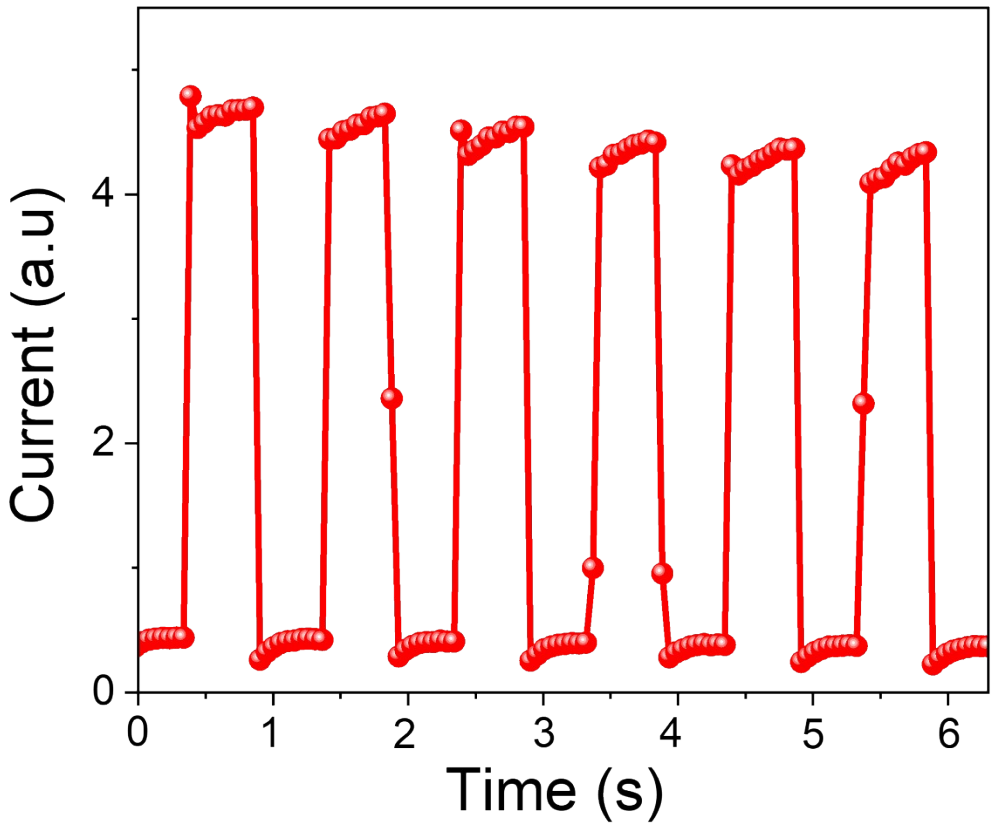


**Figure S9:** Transient photoresponse of the HT PSC–based photodetector under periodic light on/off illumination at a fixed bias.

**Table S1: Perovskite Single Crystal Carrier Mobility Benchmark for SCLC method**

| year | Perovskite Material | Temperature ( C ) | Morphology | Mobility ($Cm^2/V.S$ | Reference | Type of SCLC |
|---|---|---|---|---|---|---|
| 2015 | $MAPbBr_3$ | Room-temp. slow cooling | Bulk | 38 | *Science 347, 519–522 (2015)* | Vertical |
| 2015 | $MAPbBr_3$ | 80 | Bulk | 24 | *Nat. Commun. 2015, 6, 7586* | Vertical |
| 2016 | $MAPbBr_3$ | 90 | thin film | 15.7 | *J. Am. Chem. Soc. 2016, 138, 50, 16196–16199* | Vertical |
| 2017 | $MAPbBr_3$ | 90 | Single crystal thin film | 23.7 | *Chem. Commun., 2017,53, 5163-5166* | Vertical |
| 2017 | $MAPbI_3$ | 180 | Single Crystal thin films | 45.64 | *Nat Commun 8, 15882 (2017).* | Lateral |
| 2021 | $MAPbBr_3$ | 80 | Single crystal thin film | 13 | *ACS Energy Lett. 2021, 6, 1087−1094* | Vertical |
| 2021 | FAMACs | 60 | Bulk Crystal | 288.4 | *Adv. Mater. 2021, 33, 2006010* | Vertical |
| 2021 | $MAPbBr_3$ | 40 | Bulk Crystal | 115 | *Nanoscale, 2021,13, 8275-8282* | Vertical |
| 2020 | $MAPbBr_3$ | 75 | Thin single crystal | 97 | *Mater. Today Phys. 2020, 14, No. 100240.* | Vertical |
| 2020 | $MAPbBr_3$ | 110 | Thin single crystal | 1.16 | *Nature communications 2020, 11, 274* | Lateral |
| 2018 | $MAPbBr_3$ | 36 | Bulk | 89.09 | *Cryst. Growth Des. 2018, 18, 11, 6652–6660* | Vertical |
| 2021 | $MAPbBr_3$ | Room Temperature | Microwire | 36 | *J. Mater. Chem.C, 2021,9, 4771* | Vertical |
| 2024 | $MAPbBr_3$ | Room Temperature | Bulk | 185.86 | *Advanced Science 2024, 11, 2400150* | Vertical |
| 2025 | $MAPbBr_3$ | -18 | Thin Single crystal | 541 | *This work* | Lateral |

Reference

(1) Steele, J. A.; Lai, M.; Zhang, Y.; Lin, Z.; Hofkens, J.; Roeffaers, M. B.; Yang, P. Phase transitions and anion exchange in all-inorganic halide perovskites. *Accounts of Materials Research* **2020**, *1* (1), 3-15.

(2) Schwartz, R. W.; Schneller, T.; Waser, R. Chemical solution deposition of electronic oxide films. *Comptes Rendus Chimie* **2004**, *7* (5), 433-461.

(3) Kumar, S. G.; Rao, K. K. Polymorphic phase transition among the titania crystal structures using a solution-based approach: from precursor chemistry to nucleation process. *Nanoscale* **2014**, *6* (20), 11574-11632.

(4) Saidaminov, M. I.; Abdelhady, A. L.; Maculan, G.; Bakr, O. M. Retrograde solubility of formamidinium and methylammonium lead halide perovskites enabling rapid single crystal growth. *Chemical communications* **2015**, *51* (100), 17658-17661.